Cold Regions Science and Technology 76–77 (2012) 44–51

Contents lists available at SciVerse ScienceDirect

Cold Regions Science and Technology

journal homepage: www.elsevier.com/locate/coldregions

Decohesion with refreezing

Kara Peterson [a,1], Howard Schreyer [b], Deborah Sulsky [c,*]

[a] Sandia National Laboratories, Albuquerque, NM, United States
[b] Department of Mechanical Engineering, MSC01 1150, 1 University of New Mexico, Albuquerque, NM 87131, United States
[c] Department of Mathematics and Statistics, MSC01 1115, 1 University of New Mexico, Albuquerque, NM 87131, United States

ARTICLE INFO

Article history:
Received 14 April 2011
Received in revised form 4 August 2011
Accepted 4 August 2011

Keywords:
Decohesive constitutive model
Sea ice
Fracture
Refreezing
Gap closure

ABSTRACT

In a previous paper, an elastic-decohesive model was developed for sea ice. Unlike previous models, orientation and displacement discontinuity associated with lead opening are specifically predicted. However, over the course of a season a specific lead may open and close several times with significant implications related to ice production and heat flux. The focus of this paper is to indicate, in a generic manner, how the formation of new ice by freezing within a lead and the recovery of tensile strength by the freezing of ridges can be accommodated easily within the decohesive structure. A sample simulation is provided to show the implications of these additional terms on ice production over several cycles of lead opening and closing.

1. Introduction

In the winter, sea ice acts to insulate the warmer ocean water from the colder atmosphere. Especially when constrained by the shore, the ice cover continuously breaks up and refreezes when forced by oceanic currents or atmospheric winds. The leads, or cracks in the ice, can be kilometers wide and up to hundreds of kilometers long. The importance of leads in modeling sea ice is well known. New ice is formed primarily in leads where open water, exposed to the cold atmosphere, freezes quickly. As leads close, ice piles up into pressure ridges, or is forced down into keels, creating thicker ice. In addition, the greater albedo of the ice compared to the water results in more reflected solar radiation and cooler ice, sea, and air surface temperature. Climate simulations strive to capture these important effects of leads.

Current sea-ice models have three major components. The first component models the ice dynamics, governed by the momentum equation. The forces acting on the ice are drag from the wind and ocean, Coriolis forces, gravitational effects from the sea surface tilt, and internal ice forces that follow a constitutive model. The second component models ice thermodynamics, and is governed by a heat equation describing the temperature of the ice and snow through the thickness. The third component is an ice thickness distribution. The ice thickness distribution is a subgrid parameterization of the spatial heterogeneity of the ice thickness and accounts for redistribution of ice due to lead opening and closing. Thus, the constitutive model is one piece of a comprehensive ice model which accounts for the internal forces in the ice. These forces are responsible for the observed deviation in ice motion from free drift and, as noted, are especially important in the winter.

To account for the presence of leads, a decohesive constitutive model was developed for predicting the initiation and opening of leads in the Arctic ice (Schreyer et al., 2006). Once the existence of leads is taken into account, the remaining motion of the ice in the central Arctic ice pack has small deformations and is appropriately described as elastic. The phrase Òelastic-decohesiveÓ is used to describe this model of the dual continuum–discontinuum aspects of the behavior of Arctic ice. Several features were designed into the model. First, the model was constructed to predict the observed features of transition from brittle failure under tensile to moderate values of compression, to mixed modes of failure under larger compression, and to a plastic-like faulting under large confinement (Schulson, 2004). The various modes of failure occur in the model, depending on the stress state in the material. In other words, the predicted mode of failure depends on the state of stress, a feature not contained in most other models. Where the transitions occur in stress space depends on the material parameters and can be adjusted based on empirical data. Second, the model can handle multiple cracks at a point, and therefore can predict crack branching. Third, the numerical implementation of the model is accomplished similarly to standard plasticity models. A final aspect of the model is the ability to build in initial planes of weakness that may be due to pre-existing, partially frozen leads, for example. Initial tests of the model on a regional

* Corresponding author.
E-mail address: sulsky@math.unm.edu (D. Sulsky).

[1] Sandia National Laboratories is a multi-program laboratory managed and operated by Sandia Corporation, a wholly owned subsidiary of Lockheed Martin Corporation, for the U. S. Department of Energy's National Nuclear Security Administration under Contract DE-AC04-94AL85000.

0165-232X/$ – see front matter © 2011 Elsevier B.V. All rights reserved.
doi:10.1016/j.coldregions.2011.08.002

simulation of the Beaufort Sea show that the model is able to capture the qualitative and statistical behavior of localized deformation seen in satellite observations (Sulsky and Peterson, in press). This constitutive model is described in detail in Section 2.

Preliminary tests on basin-scale simulations of the Arctic, over a season or more, indicate that more opening and fracture of the ice is predicted than that which is calculated by processing satellite images. Sulsky and Peterson (in press) also note more fractures in their regional model. We postulate that a primary reason for these results is that in the current model, leads can close mechanically but their strength is not adjusted if they close and refreeze. This paper introduces modifications to the elastic-decohesive model to account for this aspect of ice behavior. In the next section of the paper, we review the elastic-decohesive model to date. In Section 3, we address the new model features and then in Section 4 we illustrate, in numeric examples, the implication of these features. Finally, in Section 5 we give concluding remarks.

2. The elastic-decohesive model

The ice is modeled as elastic until a stress threshold is reached, in which case the ice can fail and form a lead. For the purposes of modeling sea ice, a two-dimensional, plane-stress description of failure has been formulated assuming cracks occur in the plane. The envelope of failure points in stress space is described by a failure function, $F_n(\sigma, \mathbf{n})$ where $F_n<0$ implies no failure, $F_n=0$ implies evolving failure and $F_n>0$ is not allowed. This function is analogous to a plastic yield function in plasticity theories. The subscript n on F_n indicates a separate failure function for each potential crack orientation, and F_n depends on the stress σ, and the unit normal $\mathbf{n}$ to the crack surface. To consider all possible failure directions, a general failure function F is defined as $F=max_n F_n$.

Many classical failure criteria, such as the Rankine, Tresca and Mohr–Coulomb criteria, are expressed in terms of the traction on the failure surface (i.e., crack surface). If an associative flow rule is used, then the Rankine condition results in an opening mode and can be considered to model brittle failure. With associativity, the Tresca criterion results in a shear mode and can be considered as a model for ductile failure. When other features are added, both opening and shear can occur, resulting in mixed-mode failure. The elastic-decohesion model extends these classic criteria by adding two new features: (1) a modification of the Rankine criterion for brittle failure to allow for the possibility that a compressive stress component may lower the resistance of the material to brittle failure, and (2) a transition from brittle to ductile failure within one criterion. If a local basis consisting of $\mathbf{n}$, the unit normal to the crack, and $\mathbf{t}$, a unit vector tangent to the crack, is introduced, then the traction on the failure surface has normal component $\tau_n=\mathbf{n}\cdot\sigma\cdot\mathbf{n}$ and tangential component $\tau_t=\mathbf{t}\cdot\sigma\cdot\mathbf{n}$. The remaining component of stress in this basis (within the plane of the ice sheet) is $\sigma_{tt}=\mathbf{t}\cdot\sigma\cdot\mathbf{t}$. The brittle decohesion function is defined as follows

$$B_n = \frac{\tau_n}{\tau_{nf}} - f_n\left[\frac{1-\langle-\sigma_{tt}\rangle^2}{f_c'^2}\right], \quad \text{where } \langle x\rangle \equiv \begin{cases} x & x\geq 0 \\ 0 & x<0 \end{cases}. \tag{1}$$

Material parameters are τ_{nf}, the tensile or normal failure stress and f_c' which denotes the failure stress in uniaxial compression. For the moment, take $f_n=1$. The new criterion for brittle failure is $B_n=0$. The Macaulay bracket is used to activate the normal component of stress σ_{tt} only if it is negative. If the term involving σ_{tt} were absent then failure would occur when the normal traction on the surface reaches the threshold τ_{nf}, which is the Rankine criterion. With the σ_{tt} term, this criterion is analogous to the Rankine criterion in that failure occurs in the direction of maximum principal stress, but the critical value of the normal traction component is potentially reduced when σ_{tt} is compressive. The criterion allows for failure even if τ_n is negative, and it is this aspect of the model that allows compressive brittle failure.

Next, brittle and ductile aspects of failure are included by defining the failure function as

$$F = \max_n F_n \qquad F_n = \frac{\tau_t^2}{\tau_{sm}^2} + e^{\kappa B_n} - 1. \tag{2}$$

To gain some understanding of this form for the failure function, examine some special cases. Suppose the normal component of traction is a large negative value ($\tau_n\to-\infty$) and the other normal component of stress is zero ($\sigma_{tt}=0$) so that $B_n\to-\infty$ then Eq. (2) reduces to $\tau_t^2=\tau_{sm}^2$ for $F_n=0$. Therefore, the additional material parameter, τ_{sm}, is the failure stress in shear when the normal component of traction is large and compressive. Let the failure stress in shear for an unconfined body be denoted by τ_{sf}. Under the conditions $\tau_n=0$, $\sigma_{tt}=0$, and $f_n=1$, we have $B_n=-1$. For these conditions, we expect pure shear failure and want $F_n=0$ when $\tau_t^2=\tau_{sf}^2$. So we choose κ such that $e^{-\kappa}=1-(\tau_{sf}^2/\tau_{sm}^2)$. Notice that if $\tau_{nf}\to\infty$ and $f_c\to\infty$ then the criterion $F=0$ becomes the shear criterion of Tresca. Fig. 1 shows a sketch of the decohesion failure envelope in stress space. This function is analogous to a yield function in plasticity theories. The solid line represents the failure envelope $F=0$. Along this solid line, the black arrows indicate the direction of maximum principal stress and the gray arrows indicate the normal to the crack surface. Under brittle failure the normal to the crack is in the direction of maximum principal stress. Under ductile and mixed-mode failure the normal to the crack is at an angle to the direction of maximum principal stress, with two orientations of the crack possible. Of the two, the orientation that preserves the sense of local rotation is chosen. The transition from brittle to ductile failure occurs at a point along the failure envelope determined by the ratio of τ_{nf} to τ_{sf}, and thus is a material property.

This failure envelope describes the model for lead initiation in the ice. Once the beginning of a crack has been identified, the evolution of the lead is required. The term *decohesion* or *cohesive crack* model refers to the reduction of the traction on the crack as the crack opens. Decohesion is included in the model by introducing a softening parameter, analogous to equivalent plastic strain in plasticity models, that drives the traction to zero as a crack continues to open. A dimensionless parameter, f_n in Eq. (1), starts with a value unity for undamaged material and reduces to zero as u_n, the normal component of the jump in displacement, increases from zero. The crack is considered completely open when u_n reaches the material-dependent value u_0, at which point the traction on the crack surface has been reduced to zero and a free surface is thus formed. Accordingly, we set

$$f_n = \langle 1-u_n/u_0\rangle. \tag{3}$$

The displacement discontinuity evolves according to a normal flow rule

$$\dot{u}_n = \dot{\omega}\frac{\partial F}{\partial \tau_n} \qquad \dot{u}_t = \dot{\omega}\frac{\partial F}{\partial \tau_t}, \tag{4}$$

where a superposed dot indicates a time derivative. The displacement discontinuity is regularized into an effective decohesion strain, analogous to plastic strain,

$$\dot{e}_{nn}^d = \dot{u}_n/L \qquad \dot{e}_{nt}^d = \dot{u}_t/2L \qquad \dot{e}_{tt}^d = 0 \tag{5}$$

where L is a measure of the cell size in numerical simulations. (The value of L is chosen so that the physically correct energy is dissipated during fracture.) The stress is a function of the elastic strain $\mathbf{e}-\mathbf{e}^d$. Thus, as a specimen of ice is loaded, we typically begin with $F<0$; the

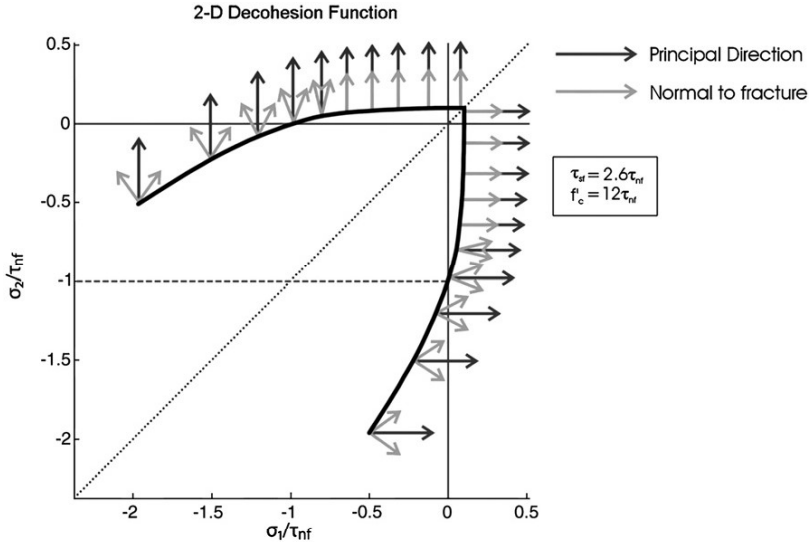

Fig. 1. Failure envelope in principal stress space for the elastic-decohesive model.

stress is inside the failure envelope. We assume each loading step is elastic, giving a trial stress state. If the trial stress is outside the failure envelope ($F>0$) then a jump in displacement is introduced to bring F back to zero. This procedure is identical to standard solution procedures for plasticity. The result is that as a crack opens we predict the amount of both the normal and tangential opening. Once a free surface has formed, the jump in displacement can continue to grow if the crack surfaces continue to separate, and the traction on the surface remains zero.

At each loading step we find the critical direction **n** for which F is largest. As a crack with a particular orientation begins to open, the softening makes it likely that this orientation will remain the critical direction. However, it is possible that a changing stress state will make another direction critical, in which case a second crack can form intersecting the first. In this manner, the model accommodates multiple cracks at a point. If weak areas are known to exist in the ice, the softening parameter f_n can be initialized with a value less than one to account for this information.

3. Refreezing

Our previous work, outlined in the last section, focuses on the prediction of lead formation. The model indicates the level of stress needed to form a lead. In addition, the model provides the orientation of the lead and tracks the amount of lead opening in terms of both the normal and tangential components of displacement associated with the displacement jump. The model above also allows for lead closure, but with no resistance to that closure. That is, once a lead is fully formed and the crack is defined by two free surfaces, those surfaces are free to move – either to open more or close, as conditions permit. However, as new ice is formed in an open lead, we expect the ice strength to begin to recover, and to resist further opening or closing of the lead. When the new ice is thin, the strength of the new ice is negligible in either tension or compression. With sufficient time and favorable thermodynamic conditions, a combination of freezing or crushing of ice in the lead builds up the thickness and the strength. This section of the paper focuses on the mechanical aspects of strength recovery due to refreezing and presents simple adjustments that extend the decohesive constitutive model to include physics of Arctic ice not present in the original model.

The thermodynamic model described in Appendix A tracks thickness changes in the ice due to freezing or melting. Moreover, the range of ice thickness within a computational cell that can be created by freezing and ridging of ice is tracked by the ice thickness distribution model of Appendix A. When a lead is formed, open water is created and when a lead closes, ridging occurs and ice is redistributed from thinner to thicker ice in the thickness distribution. We assume that the thinnest ice in the ice thickness distribution occurs in a lead if one, or more, exists within a computational cell.

To enhance the model, we consider that a lead can regain its strength if the lead closes and the free surfaces come together for a sufficient duration to refreeze. A change in strength in the ice model is reflected by replacing the softening function f_n in Eq. (3) with $\hat{f}_n$ where

$$\hat{f}_n = \begin{cases} \langle 1 - u_n / u_0 \rangle & \text{if the lead is opening or closing} \\ f_n^* & \text{if a lead has closed and } u_n \le u_0 \end{cases}. \tag{6}$$

The new parameter, f_n^*, only becomes active once a lead has opened and closed. In intact ice, we start with no opening, $u_n = 0$, and $f_n^* = 0$. Thus, we have the original model where $\hat{f}_n = f_n = \langle 1 - u_n / u_0 \rangle$. A lead is formed when u_n reaches u_0 and the lead typically opens to a distance $u_n > u_0$. The original softening function, f_n, is zero once $u_n \ge u_0$. The value of f_n^* is unchanged until a ridge is formed. Suppose a lead opens to a width $u_n >> u_0$, ice now begins to form in the lead as water freezes. Further suppose conditions change so that the lead begins to close. If the lead closes completely, then u_n will return to a value equal to u_0. During this process, ridging takes place. Under stable conditions, the ridge will freeze and the ridged ice in the lead should regain strength. To accomplish this strengthening of the ice, an evolution equation for the growth of f_n^* is proposed. Its value should start at zero and increase as freezing occurs. If $f_n^* < 1$, the inherent strength as given by $\hat{f}_n$ is less than the original material, but greater than the strength of the fully opened lead. Once $f_n^* = 1$, the lead has healed completely. The parameter f_n^* does not increase beyond unity because ice immediately adjacent to the ridge will govern failure. At this point the lead is closed, u_n and f_n^* are reset to zero, and the process can repeat.

Starting from the value zero, the rate of increase of strength, $\dot{f}_n^*$, is assumed to depend on the temperature difference between the air and the ocean. The evolution equation for enhanced strength is intended to be a representative example of how such a feature can be incorporated into the formulation. Additional considerations such as desalination, width and depth of the ridged ice, and wind may require

a modification to the proposed form. As the strength increases, it is possible that the rate decreases. Moreover, the strength should never exceed the original strength. Therefore, the following evolution equation is proposed

$$\dot{f}_n^* = \frac{A(T)}{(1+f_n^*)^m} \qquad f_n^*(0) = 0. \tag{7}$$

In this evolution equation, the parameter $A(T)$ is a ratio of the temperature difference between the ocean and air and a given reference temperature T_{ref} and takes the following form

$$A(T) = \frac{T_{ocean} - T_{air}}{T_{ref}}. \tag{8}$$

The constant T_{ref} and the exponent m set the time scale over which f_n^* returns to the value unity.

Fig. 2 displays the evolution of the strength function for an exponent $m=5$ and for three constant values of $A(T)$. The values of $A(T)$ used in this figure could correspond to a reference temperature $T_{ref}=20$ °C and temperature differences between the ocean and atmosphere of 20 °C, 40 °C, and 60 °C respectively. For these parameters the ice regains its strength within 3 to 11 days. Changes in the reference temperature change the typical length of time needed for the ice to regain its strength, and thus the model can be adjusted to fit observations.

A key point is that this evolution equation allows the temperature to vary in any manner. Additionally, a new lead can be formed at any time based on the current strength. If either a completely refrozen lead whose strength has completely recovered, or a partially refrozen lead whose strength is still lower than the original value, is subject to new winds or ocean currents that cause it to reopen, then the strength recovery is reset and the process described above is repeated. We expect that if a lead opens and closes repeatedly without refreezing then more ice is formed than if a lead opens and closes once with the ridged ice refreezing and regaining strength. These scenarios are explored through specific numeric examples in the next section.

4. Numeric examples

In order to illustrate the behavior of the elastic-decohesive constitutive model with and without strength recovery due to closure and refreezing of leads, we perform a simple calculation using the Material-Point Method (MPM). MPM is a numerical technique that combines Lagrangian particles with a background grid (Sulsky et al., 1994, 1995). A description of the application of MPM to sea ice is given in Sulsky et al. (2007) and Sulsky and Peterson (in press). The Lagrangian particles, or material points, carry mass, velocity, stress, ice thickness, and other material parameters and internal variables for the constitutive and thermodynamic models, as well as the thickness distribution. The Lagrangian representation allows for these quantities to be transported with the material motion in a natural manner. Material-point properties are mapped to the background grid for the solution of the momentum equation at each time step. The model used in this analysis combines the elastic-decohesive constitutive model used in the momentum equation for the ice dynamics, with an energy conserving thermodynamic implementation for ice growth and melt, and a five category ice thickness distribution incorporating ridging. A brief summary of the governing equations for each of these components are found in Appendix A.

For the example calculation a block of ice 1050 km long and 600 km wide with an initial region of decohesion down the center, at $x=0$ km, is forced by cyclic atmospheric winds. The computational domain is larger than the block of ice and is divided into a 1150×700 km background grid, which is composed of square cells of dimension 50 km. The ice region contained within the background grid is made up of material points. The region of initially weakened ice in a line through the center of the ice region is initialized by setting the normalized decohesion opening (u_n/u_0) equal to 0.8 and with the normal to the crack surface set to the x-direction. Therefore, the initial strength function is $\hat{f}_n = 0.2$ along this line. An overview of the computational domain displaying initial values of normalized decohesion opening magnitude are shown in Fig. 3. The initial average ice thickness is approximately 2.6 m for each material point and is calculated by summing over the five ice thickness categories at each material point. The parameters used in the decohesion algorithm are given in Table 1.

The simulations are run for three months with a time step of 100 s. For the strength recovery algorithm, the parameters chosen result in a strength evolution over time as shown in Fig. 2 with $A=2$. This value allows stationary ice to regain its strength in about five days. Note that the parameter A depends, in general, on the temperature difference between the ocean and the atmosphere and would therefore vary seasonally over a longer calculation.

The atmospheric winds are set to pull then push the block of ice in the horizontal direction to open and close the crack down the center. This forcing is accomplished by setting the wind velocity to cycle, putting the ice in tension for a period of 5 days, compressing the ice for 10 days, and pausing for 10 day intervals of zero velocity between the active periods to allow for ice growth. A plot of the velocity cycle as a function of time for a point on the right side of the domain for the first set of simulations is shown in Fig. 4a and a plot of the atmospheric wind velocity over the domain on day two is shown in Fig. 4b.

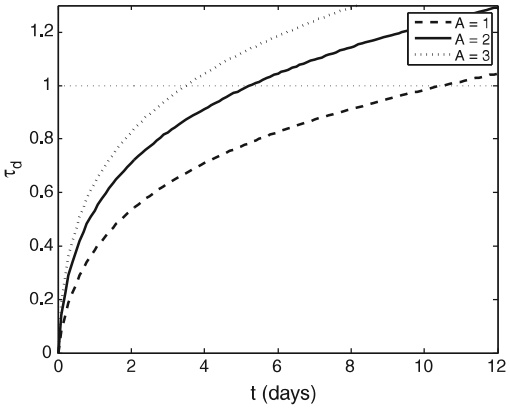

Fig. 2. Time evolution of the strength parameter, f_n^*, due to refreezing for constant ocean-air temperature differences. In practice, the parameter is not allowed to increase beyond unity.

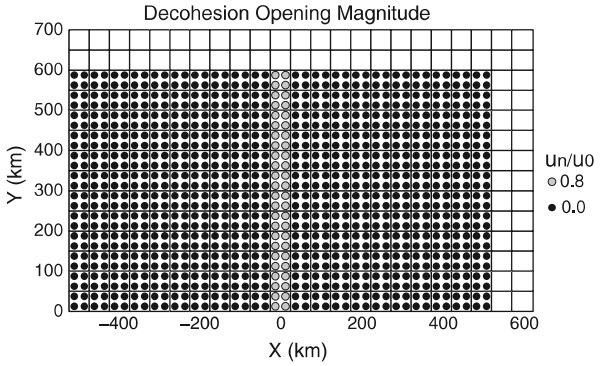

Fig. 3. Initial normalized decohesion opening. A nonzero value of 0.8 is initialized in the central region to model a pre-existing weakened area.

Table 1
Decohesion parameters used in the simulations.

Variable	Value	Description
τ_{nf}	2.5 kPa	Tensile strength
τ_{sm}	6.0 kPa	Shear strength
f_c'	12.5 kPa	Compressive strength
u_0	4 km	Minimum decohesion opening
m	5	Exponent in strength factor

Table 2
Atmospheric and oceanic forcing.

Variable	Value	Description
F_{lw}	187.5 W/m^2	Downwelling longwave flux
F_{sw}	0 W/m^2	Downwelling shortwave flux
T_{air}	−38 °C	Air temperature
Q	5×10^{-5}	Specific humidity
F_{snow}	6×10^{-6}	Snow flux (precipitation)
SST	−1.96 °C	Sea surface temperature
SSS	32 ppt	Sea surface salinity

The ocean current is assumed to be zero, but an ocean drag depending on the ice velocity is still applied. The atmospheric and oceanic forcing has a magnitude consistent with typical forcing over winter months in the Arctic. The values for the oceanic and atmospheric forcing parameters are given in Table 2.

The effect of adding the strength recovery algorithm for closing leads in the simulations can be seen by plotting the normalized decohesion opening in the x direction for a point in the center of the ice domain as a function of time, as shown in Fig. 5a. A material point is chosen in the initially weakened ice and its decohesion history is displayed in the figure. The point starts with a normalized decohesion opening equal to 0.8. Without strength recovery, the ice can freely open and close and the decohesion opening cycles in response to the cyclic wind. The lead opens to a scaled value of 6 over the first 5 days, stays roughly constant over the next 5 days as the winds die down, and then closes within 5 days when the winds reverse. Since the ice is still fractured, when the wind changes, the lead can reopen and repeat the previous pattern. If strength recovery is added, the first tension and compression cycle is identical. However, once the ice has compressed in the simulation with strength recovery, the crack heals and the full strength is regained over the ten days between the last compression portion of the cycle and the new tension portion of the cycle. Once this happens, the forcing in this simulation is never enough to reinitiate decohesion and the lead does not reopen. Therefore, on day 15 in Fig. 5a the calculations begin to differ such that the ice with strength recovery is no longer able to pull apart under the given tension. The corresponding evolution of the strength factor is shown in Fig. 5b. Without strength recovery, the strength factor starts at 0.2 and then decreases to zero as the lead opens. The strength factor then remains at zero for the duration of the simulation. With strength recovery, the strength factor increases from zero back to one and the ice remains at full strength for the duration of the simulation. Note that the strength factor is only nonzero for points that have previously undergone decohesion and have closed sufficiently to allow refreezing.

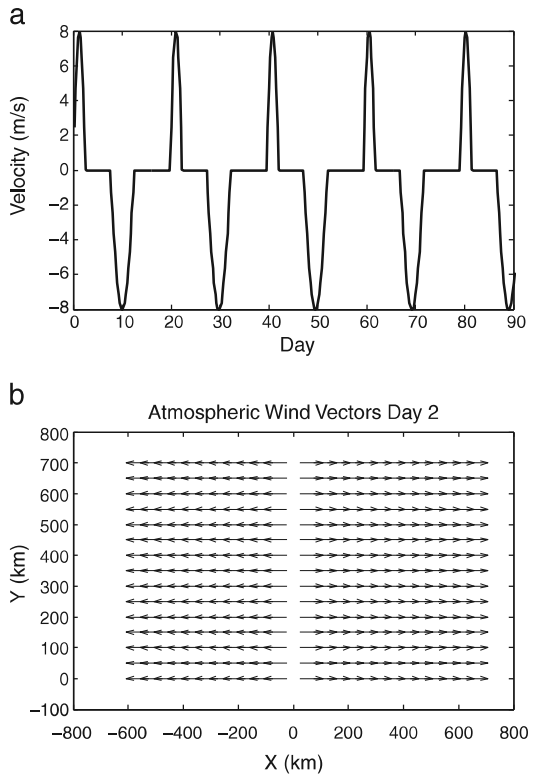

Fig. 4. (a) Atmospheric wind in the x direction as a function of time for a point to the right of the center of the block of ice. For points to the left of the center the wind velocity is equal and opposite. (b) Atmospheric wind vectors over the calculation domain on day 2 near the peak of the velocity cycle.

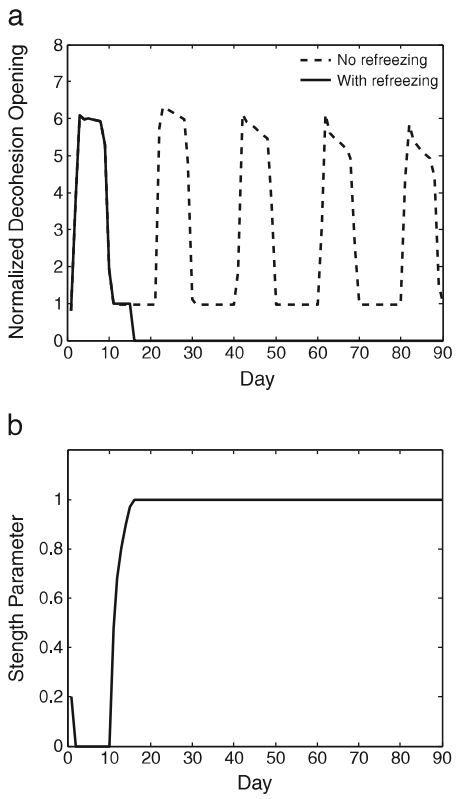

Fig. 5. (a) Normalized decohesion opening as a function of time for a point in the center of the initial lead. The dashed line is for the case of the original elastic-decohesive formulation with no strength recovery in leads and the solid line displays the case where refreezing and strength recovery in the lead is included. (b) Evolution of the strength factor as a function of time when strength recovery is included, for the same point.

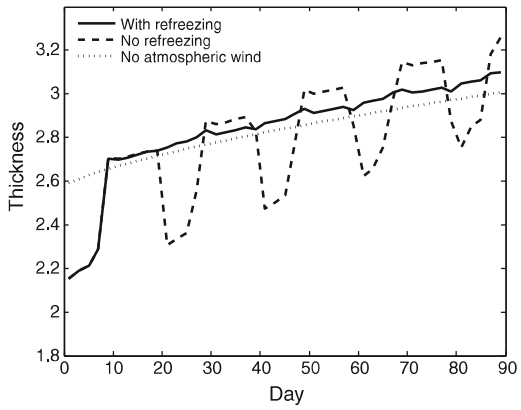

Fig. 6. Thickness at a point near the center of the ice domain for three cases: with strength recovery in the lead, original formulation without strength recovery, and without atmospheric winds.

To examine how the strength recovery algorithm effects ice production within a lead, we examine the average thickness for a point near the center of the ice domain and plot it as a function of time in Fig. 6. The dashed line in the figure is the original model where the ice in the lead does not regain strength over time. The average thickness cycles with the applied atmospheric winds. When the winds pull the ice apart, open water is created, and the average thickness goes down. However, new ice is formed in the open lead and grows quickly while the wind forcing is stopped. When the winds next compress the ice, ridges form from the newly grown ice and the average thickness goes up. Over time, this cyclic motion increases the peak average thickness. Since thin ice grows more quickly than thicker ice, this cyclic behavior of the lead will eventually produce more ice than will be produced in a region of ice without a lead that is exposed to the same thermodynamic forcing. Another simulation, labeled in Fig. 6 as "No atmospheric wind" and plotted with a dotted line, shows this case where the initial configuration of ice is the same, but no atmospheric wind forcing is applied to open a lead. As can be seen, the increase in peak thickness due to thermodynamic growth of the open water in a lead that is allowed to reopen and then close and ridge, outpaces the thermodynamic growth of an intact region of ice. In the case where strength recovery due to refreezing is included, an initial ridge is formed during the first compressive cycle and then that ice increases slowly in thickness commensurate with thermodynamic growth of an intact region.

As expected from the results for the ice thickness at a material point, the total volume of ice over the simulation is also altered by the strength recovery algorithm. The total ice volume is the area times the thickness, summed over the domain and is shown in Fig. 7a as a function of time. The total volume increases over time in all cases due to ice growth caused by the atmospheric and ocean heat flux applied in the simulations. To see the impact of strength recovery in a lead more clearly, the volume increase in the case of the intact region (with no atmospheric winds applied) is subtracted from the other two simulation results. Thus, Fig. 7b measures the change in volume attributable to the cycling of the lead. Clearly, the continued opening and closing of a lead causes an increase in ice volume as ice forms in the lead and is crushed into a ridge with each cycle. This increase in ice volume is larger by about 50% than the ice volume formed when the lead regains strength after closing and refreezing and does not reopen.

The thickness distributions at a point near the center of the domain for each of the cases previously considered are shown in Fig. 8. Note that at the final time the thickness distribution for the original formulation without strength recovery is shifted more towards thicker ice. This result is consistent with the average thickness over the domain being larger when the lead is allowed to cycle without

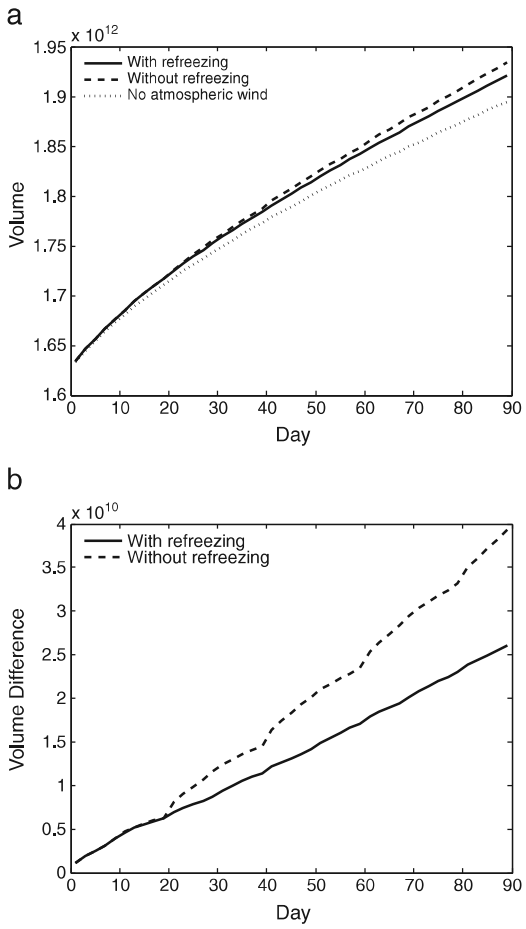

Fig. 7. Ice volume versus time over the entire ice domain (a) for three cases: with strength recovery in the lead, original formulation without strength recovery, and no atmospheric winds and (b) for the strength recovery and original formulation, showing the difference of each from the case of no atmospheric wind.

resistance. The thickness distribution when strength recovery is included is similar to the simulation with no atmospheric winds where the lead is never formed. Again, this picture is to be expected based on the calculations of ice thickness and volume changes.

5. Summary

An elastic-decohesive model was developed to predict lead opening and the orientation of the lead in simulations of Arctic sea ice. In previous work, the model was shown to reproduce qualitative and statistical properties of lead formation in a regional study of the Beaufort Sea. This paper suggests a modification to the model in order to add an important element for predicting the closure of leads and the formation of fresh ice. For this modification an evolution equation is provided to model the recovery of strength of a closed lead due to refreezing within ridged ice. With a reversal of wind, a ridge with no strength will open and fresh ice will form in the lead. However, with a recovery of strength, the ridge may not open and, consequently, no new ice is formed. This second aspect is particularly important for an accurate prediction of the formation of fresh ice in leads, and ultimately for correctly predicting ice production in climate simulations.

Two simulations were performed, with and without strength recovery due to refreezing. The parameters were chosen to bracket two possible extremes and to illustrate the contribution of refreezing

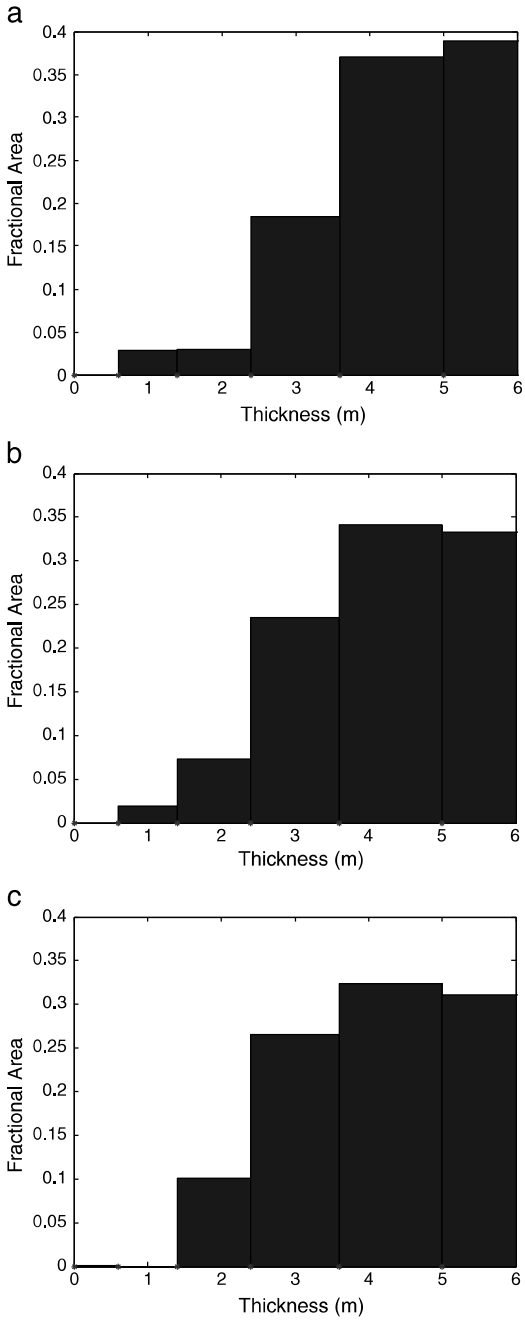

Fig. 8. Ice thickness distribution at the final time for (a) original formulation without strength recovery, (b) with strength recovery in the lead, and (c) with no atmospheric wind.

to the ice model. In the first simulation, the strength is not allowed to recover. The lead can open and close without resistance. Repeated, cyclic opening and closing of the lead produces more ice relative to the second simulation where the strength of the ice recovers when a ridge is formed. The impact of the modified model on global Arctic simulations remains to be seen, and is the subject of future work.

Acknowledgements

The authors wish to acknowledge with fondness and appreciation that this work was initiated because of the persistence of Max D. Coon whose extensive knowledge of Arctic ice provided the insight on which many aspects of the models described in this paper are based. This work was partially supported by the National Science Foundation under grant ARC-1023667. Additional support for KP from the NNSA Climate Modeling and Carbon Measurement project and a Laboratory Directed Research and Development award are gratefully acknowledged.

Appendix A. Equations of motion

The mathematical model of sea ice is derived from considering the balance of linear momentum which is expressed by the following equation (Coon et al., 1974)

$$m\frac{dv}{dt} = F^{\text{int}} + F^{\text{ext}}. \tag{A.1}$$

In this equation, the time derivative is a material-time derivative, $d/dt = \partial/\partial t + \mathbf{v}\cdot\nabla$, where $\mathbf{v} = \mathbf{v}(\mathbf{x}, t)$ is the velocity field associated with the point $\mathbf{x}$ at time t. This equation is derived by assuming the ice properties are constant through the thickness. Integration through the thickness leaves a two-dimensional equation describing motion in the plane of the ice. The quantity m is the ice mass per unit area, and $F^{\text{int}} = \nabla\cdot\overline{h}\sigma$ is the force due to variation in internal ice stress, given by the divergence of the stress tensor, σ, times the ice thickness, $\overline{h}$. External forces are described by the vector $\mathbf{F}^{\text{ext}}$ which include Coriolis forces, air stress and water stress, and effects of sea surface tilt. Ice thickness can change due to the thermodynamic processes of melting and freezing, or mechanical processes such as lead or ridge formation. Since numeric climate simulations still must use large computational elements, within each element there is a distribution of ice thickness. The quantity $\overline{h}$ is the average thickness. A subgrid scale model for the distribution of ice thickness, $g(\mathbf{x}, h, t)$, keeps track of the evolution of ice thickness within an element (Thorndike et al., 1975) according to the equation

$$\frac{dg}{dt} + (\nabla\cdot\mathbf{v})g + \frac{\partial(fg)}{\partial h} = \psi. \tag{A.2}$$

The first two terms in this equation describe horizontal transport and the changes in thickness at a point due to ice motion. The third term expresses transport in thickness space, with $f = dh/dt$ being the rate at which thickness h changes due to thermodynamic processes. Finally, ψ, describes mechanical redistribution of ice and accounts for ridge formation in converging flow or the creation of open water in diverging flow. The ridging redistribution function described in Lipscomb et al.(2007) is used in our simulations. The local average ice thickness can be computed from the distribution by integration in thickness space

$$\overline{h} = \int_0^\infty hg\ dh. \tag{A.3}$$

Freezing and melting on the top and bottom surfaces is determined by solving a one dimensional heat equation for the temperature through the thickness (Bitz and Lipscomb, 1999; Maykut and Untersteiner, 1971). The coordinate in the direction perpendicular to the plane of the ice is labeled as the z coordinate and the heat equation is

$$\rho c\frac{dT}{dt} = \frac{\partial}{\partial z}\left(k\frac{\partial T}{\partial z}\right) + \overline{\kappa} I_0 e^{-\overline{\kappa} z}. \tag{A.4}$$

The heat capacity, c, and conductivity, k, are functions of temperature and salinity, where the salinity is given by a fixed profile depending on the vertical coordinate (Bitz and Lipscomb, 1999). The quantity $\overline{\kappa}$ is the extinction coefficient, and I_0 is the solar radiation that

penetrates the upper surface. To obtain the change in thickness of the ice due to thermodynamic forcing the following balance of flux equations must be solved at the atmosphere and ocean interfaces

$$F_w - k\frac{\partial T}{\partial z} = -q\frac{dh}{dt}$$
$$F_a + k\frac{\partial T}{\partial z} = \begin{cases} 0 & T_0 = 0^\circ C \\ -q\frac{dh}{dt} & T_0 < 0^\circ C \end{cases}. \quad (A.5)$$

where the enthalpy, q, is also dependent on the temperature and salinity. Note that dh/dt at each surface is summed to obtain the rate of change in thickness, f, in the ice thickness distribution equation, Eq. (A.2). The flux at the ocean interface, F_w, is simply the heat flux from the ocean to the ice. The net flux at the atmosphere interface, F_a, is a combination of flux terms as shown in Eq. (A.6). It includes downwelling shortwave radiation from the sun, F_R, minus the fraction which is reflected based on the albedo of the surface, α, and the fraction that is transmitted through the ice, I_0. It additionally includes the downwelling longwave radiation due to atmospheric heating, F_L, and the upward longwave radiation from the ice surface, which is defined in terms of the surface temperature, T_0, the Stefan–Boltzmann constant, σ, and the longwave emissivity of the surface, ϵ_L. The final terms in the balance are the flux of sensible heat, F_s, and the flux of latent heat, F_l

$$F_a = F_R(1-\alpha) - I_0 + F_L - \epsilon_L \sigma T_0^4 + F_s + F_l. \quad (A.6)$$

In order to complete the mathematical description, a constitutive model for the stress is required. This model is the topic of the main body of the paper.

References

Bitz, C.M., Lipscomb, W.H., 1999. An energy-conserving thermodynamic model of sea ice. Journal of Geophysical Research 104 (C7), 15669–15677.

Coon, M.D., Maykut, G.A., Pritchard, R.S., Rothrock, D.A., Thorndike, A.S., 1974. Modeling the pack ice as an elastic-plastic material. AIDJEX Bulletin 24, 1–105.

Lipscomb, W.H., Hunke, E.C., Maslowski, W., Jakacki, J., 2007. Ridging, strength, and stability in high-resolution sea ice models. Journal of Geophysical Research 112, C03S91.

Maykut, G.A., Untersteiner, N., 1971. Some results from a time-dependent thermodynamic model of sea ice. Journal of Geophysical Research 76 (6), 1550–1575.

Schreyer, H., Monday, L., Sulsky, D., Coon, M., Kwok, R., 2006. Elastic-decohesive constitutive model for sea ice. Journal of Geophysical Research 111, C11S26.

Schulson, E.M., 2004. Compressive shear faults within arctic sea ice: fracture on scales large and small. Journal of Geophysical Research 109, C07016.

Sulsky, D., Peterson, K., in press. Towards a new, elastic-decohesive model of Arctic sea ice. Physica D, to appear. doi:10.1016/j.physd.2011.07.005.

Sulsky, D., Chen, Z., Schreyer, H., 1994. A particle method for history-dependent materials. Computer Methods in Applied Mechanics and Engineering 118, 179–196.

Sulsky, D., Zhou, S., Schreyer, H., 1995. Application of a particle-in-cell method to solid mechanics. Computer Physics Communications 87, 236–252.

Sulsky, D., Schreyer, H., Peterson, K., Coon, M., Kwok, R., 2007. Using the material-point method to model sea ice dynamics. Journal of Geophysical Research 112, C02S90.

Thorndike, A., D., Maykut, G., Colony, R., November 1975. The thickness distribution of seaice. Journal of Geophysical Research 80 (33), 4501–4513.